Jurnal MIPA dan Pembelajarannya
e-issn: 2798-0634, email: jmipap.journal@um.ac.id

VOL	ISS	YEAR	DOI
6	4	2026	10.17977/um067.v6.i4.2026.3

INVESTIGATING THE EFFECT OF PB-AL DOPED CDS AND CDS: PB/CDS: AL HOMOJUNCTION ON STRUCTURE AND GAS SENSING PROPERTIES SYNTHESIS BY CHEMICAL BATH DEPOSITION METHOD

Azhar Mohammed Abd

Salah Al-Din Education Directorate, Ministry of Education, Tikrit, Iraq
*Corresponding author, email: a3913783@gmail.com

Keywords
Gas Sensor
Cadmium Sulphide
Chemical Bath Deposition
Nitrogen Dioxide

Abstract
In this study, thin film of undoped CdS is prepared, in addition to other films doped with Pb and Al at different concentration between 0.002M to 0.006M and CdS: Pb/CdS: Al homojunction, these films were deposited using the chemical bath deposition method on glass substrate at deposition temperature of 70°C. To analysis the structural and morphological characteristcs of (Pb, Al)-doped CdS thin films and CdS: Pb/ CdS: Al homojunction films were utilizing "x-ray diffraction, field emission scanning electron microscopy, as well as energy dispersive X-ray". The pattern of XRD showed that the pure CdS thin film had mix phase of hexagonal and cubic, which was turned to cubic structure by doping of Pb and Al. FE-SEM images reveal that the CdS thin film without doping a uniform morphology of spherical-like morphology with different size between 35.85nm to 64.18nm. The EDX analysis showed the existence of Cd, S, Pb and Al as primary elements in those films. The electrical resistance of the pure CdS thin film is rises when reacting with reducing gas, and reduces in the presence of an oxidizing gas, which demonstrates the behavior of p-type semiconductors. The resistances of Pb-doped CdS thin films are decreases upon exposure to a reducing gas, and increases in the presence of an oxidizing gases, demonstrating a n-type semiconductor behavior. Al-doped CdS thin film not causes an inversion the p-type behavior of the CdS semiconductor. Pb-doped CdS thin film at concentration of 0.004M show the highest sensitivity for both Hydrogen sulfide and Nitrogen dioxide gases 175.2% and 48.31% respectively at operating temperature of 300°C. Al-doped CdS thin film at concentration of 0.004M show the highest sensitivity for both Hydrogen sulfide and Nitrogen dioxide gases were 54.15% and 35.2% respectively at operating temperature of 200°C.

1. Introduction

Dangerous gases present in the atmosphere such as CH4, NO2, Co, NH3 and H2, this could have serious effects human health and contribute to global warming (Ramarj et al., 2022). Hydrogen sulfide (H2S) is a poisonous and flammable gas with the smell of rotten egg, it can cause symptoms such as dizziness, vomiting, nausea, and eye irritation (Verma & Gupta, 2012). H2S is formed in wastewater treatment plants, natural gas industries, coal mines, crude petroleum and biodegradation of organic waste material. Also, H2S is used in research laboratories, different chemical industries and as a gas treatment in heavy water production (Bari, Patil, & Bari, 2013). Nitrogen dioxide (NO2) is a toxic gas that have can harmfully affect human health even at very low concentrations, measured in ppb. Also, inhaling of NO2 may cause respiratory infections, pulmonary edema, asthma and bronchitis (Ramarj et al., 2022). The NO2 gas is usually generated from automobile engines, industrial processes, and fossil fuels (Yin et al., 2022). Therefore, we decided to conduct a study on the impact of CdS thin films that are doped with Pb and Al, as well as CdS: Pb/ CdS: Al thin film on the detection of (H2S) and (NO2) gases. Cadmium sulphide (CdS) is an n-type semiconductor from the IV-VI group that has a direct band gap ranging from 2.38 eV to 2.58 eV, and has cubic (metastable, Eg = 2.38 eV) or wurtzite (stable, Eg = 2.58 eV) crystal structure (Ashok et al., 2020). CdS crystallizes in two phases: the cubic phase, referred to as Zinc blende structure, and

hexagonal phase, called the wurtzite structure (Ferra-Gonzalez et al., 2014). Cadmium sulphide (CdS) thin film is regularly prepared using different techniques due to their wide range of application (Toma, Hussain, Rahman, & Syed, 2021). There are numerous method available for depositing CdS thin films using different of fabrication like, chemical vapor deposition (Bettini, Bachmann, & Shay, 1978), spray pyrolysis (Diwate et al., 2017), electrodeposition (Aliyu, Diso, Musa, & Abubakar, 2022), thermal evaporation (Faraj & Ibrahim, 2012), sputtering (Paudel, Wieland, & Compaan, 2012), physical vapor deposition (Shanmugariya & Sakthivel, 2020) and chemical bath deposition (Soonmin, 2021). One of these techniques (CBD) is easy to use and enhance deposition over a larger area at lower bath temperature (Batu & Tamasgen, 2020). Low cost, vacuum free, adherent, stable thin film (Tyagi, Rahim, Rahim, & Selvaraj, 2013), and deposition of various substances such as, titanium, soda lime glass, microscope gas slide, mica, and stainless steel (Soonmin, 2021). CdS thin films are one of semiconductor materials of considerable interest due to its widely used of technological application such as optical conductor of window solar cell and absorber (Toma et al., 2021). In optoelectronics technology, thin film of CdS is used in manufacture of light-emitting diodes (LEDs), this is attributed to its excellent luminescent characteristic (An et al., 2021), sensors, and photo detectors allow for the effective detection of environmental pollutants and hazardous gases as a result of their wide energy gap and excellent electron transport properties, visible light, in addition to ultraviolet (Hasanirokh, Asgari, & Mohammadi, 2021). In this paper preparative parameters were used to synthesized thin films among these factors are deposition time, bath temperature, PH and concentration of various reagents during the chemical bath deposition process were optimized to achieve high-quality of CdS thin films on glass substrate.

In this research, we study the influence of using different Al and Pb concentrations on CdS thin films and CdS:Pb/CdS:Al homojunction grown by the CBD method, with the aim of studding its impacts on structure, morphological, and gas sensing.

2. Method

Thin films of CdS doped with Pb and Al, as well as CdS: Pb/ CdS: Al homojunction, it was prepared using the chemical bath deposition method. Glass bases (76mm×25mm×2mm) were cleaned by using sodium hydroxide (NaOH) aqueous solution (2M) for 20 minutes, followed by immersion in a solution of hydraulic acid (HCl) at a concentration of (0.1M) for 5 minutes. Then glass substrates were cleaned by ethanol (98%). After cleaning process is complete in each solution, the substrate rinsed with distilled water. The deposition bath containing a reactive solution, is prepared by adding the materials sequentially of 30 ml of 0.1M Cadmium chloride monohydrate($CdCl_2.H_2O$), 10 ml of 2.5 M Ammonium chloride (NH4Cl2), 15 ml of 1.5 M (NH4OH) and 10 ml of 1 M Thiourea $CS(NH_2)_2$. Pb and Al doping were carried out by adding (0.002M, 0.004M and 0.006M) of lead nitrate (Pb (NO3)2) and Aluminum chloride (AlCl3.6H2O) to the main solution, were mixed together by magnetic stirrer. Then add deionized water to the reactive solution to complete a total volume of 100 ml. After a few minutes of stirring, the solution color turned yellow and became homogenous as shown in Figure 1. The prepared substrates are positioned vertically inside the deposition solution for duration of 2 hours. The temperature of reactive solution was kept at 70°C. After removing the samples from the chemical bath, they rinsed with double distilled water and subsequently dried at room temperature. The CdS:Pb/ CdS:Al homojunction was prepared in three stages: the first consisted of depositing CdS: Pb thin film on glass substrate, next two stages, the heat treatment of CdS: Pb thin film was performed in oven at ~150°C for 30 min. The third stages were used to deposit the CdS:Al on CdS: Pb thin film to achieve the CdS:Pb/ CdS:Al homojunction.

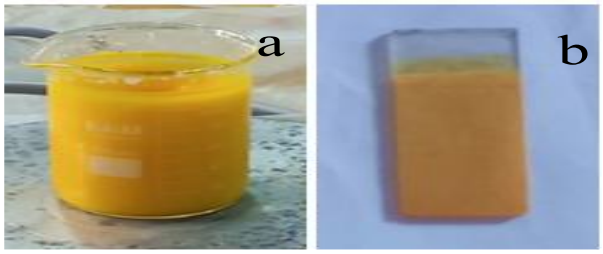

Figure 1 (a) color of the solution, (b) thin film

The structure properties of (Pb, Al)-doped CdS films and CdS: Pb/ CdS: Al homojunction films was obtained X-ray diffractometer "(XRD, Bruker D2 PHASER, with Cu-Ka radiation having wavelength λ= 1.5406A)". The morphologies of nanocrystalline of thin films were investigated using Scanning electron microscope "(SEM, EBSD-ZESS SIGMA VP Germany)". The compositional analysis

of CdS thin films doped with Pb and Al, as well as CdS: Pb/ CdS: Al homojunction films was detected by utilizing energy – dispersive X-ray (EDAX). The sensitivity (S%) of an H2S and NO2 gas sensor can be defined as follows:

$$(S\%) = \frac{R_{on} - R_{off}}{R_{0n}} \times 100 \ldots\ldots\ldots\ldots\ldots\ldots\ldots\ldots\ldots\ldots\ldots\ldots \text{for oxidizing gas (1)}$$

$$(S\%) = \frac{R_{0ff} - R_{on}}{R_{off}} \times 100 \ldots\ldots\ldots\ldots\ldots\ldots\ldots\ldots\ldots\ldots\ldots\ldots \text{for reducing gas (2)}$$

Where, R_{off} is resistance of the sensor in the air and $R_{0n}$is sensor resistance after gas exposure.

3. Result and Discusion

3.1. X-ray diffraction

Figure 2 demonstrates the XRD characteristics for the pure CdS film, CdS films doped with Pb and Al, as well as CdS:Pb/CdS:Al homojunction. CdS can be either in hexagonal phase or cubic phase or can be a mix of the two (Liu et al., 2010; Rondiya et al., 2017). The XRD patterns shows that CdS has many peaks shared between hexagonal and cubic phases. As illustrated in Figure 2, the peaks are associated with (111), (200) and (220) for cubic phase compared with standard ICD card No. 00-010-0454, but the peak corresponding to the plans (102) and (110) indicated that the phase reflects the characteristics of hexagonal crystalline shape. The result of XRD shows the main reflection peak of plane (111) located at 2θ of approximately which reveals the presence of cubic phase for CdS thin films. The effects doping of Pb and Al on crystalline structure of CdS usually causes a phase transition from mix structure to cubic phase, also notice that the diffraction peaks slightly shifted towards smaller 2θ values with Al and Pb doping which confirms that the doped Pb and Al substitutes in CdS. This due to the ionic radius is larger of Pb (1.19 Å) when compared with that of Cd^{2+} (0.97 Å). The XRD pattern shows that the decrease in the peak intensity of (111) plane when the amount of Pb(NO3)2 and AlCl3·6H2O in the solution increases. This can be attributed to a small size of the crystals (Chavez-Urbiola, Pintor-Monroy, Willars-Rodriguez, & Quevedo-Lopez, 2019).

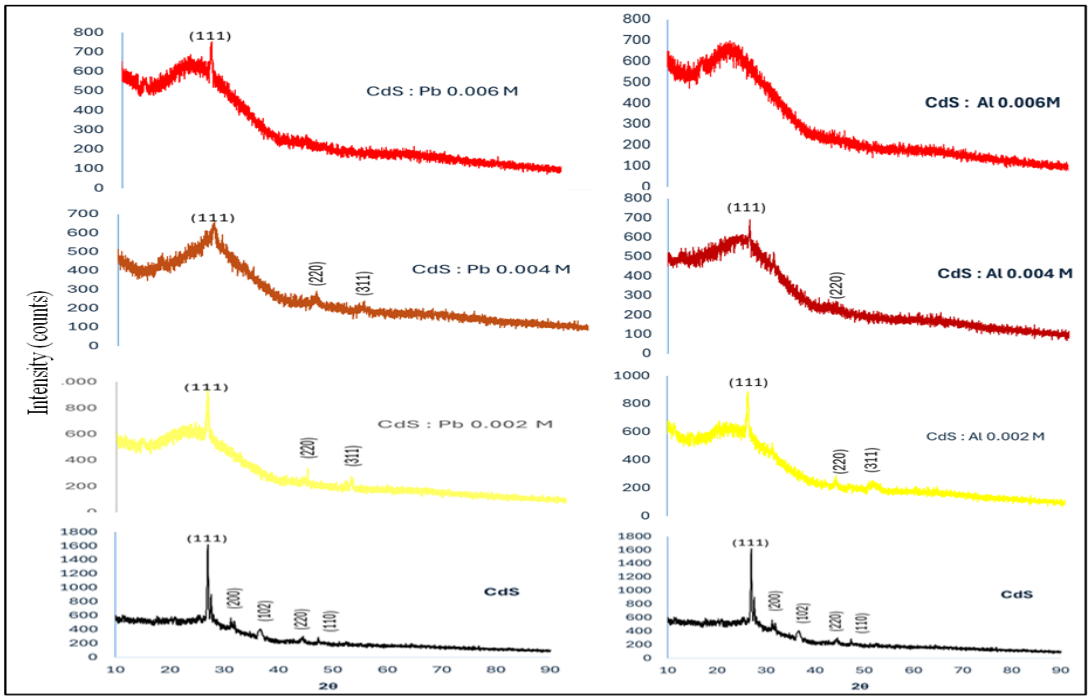

Figure 2. patterns of XRD for undoped CdS film and CdS films doped with Pb and Al at various concentration

When deposit the CdS:Al on CdS:Pb thin film, the cubic phase of CdS films doped with Pb and Al transition to the mixed structure of hexagonal and cubic. As demonstrated in Figure 3, the diffraction

peak at 2θ values 24.89 (100), 26.37 (002), 28.69 (101), 43.82 (110) and 51.15 (112) for hexagonal phase compared with standard ICD card No. 77-2306 (Muthusamy, Muthukumaran, & Ashokkumar, 2014), but the peak corresponding to the plans 26.37 (111) and 31.33 (200), 43.82 (220), 51.15 (311) and 54.4 (222) indicated that the phase belongs to cubic compared with standard ICD card No. 01-080-0019 (Jafari, Zakaria, Rizwan, & Ghazali, 2011). The thin films of CdS doped with Pb and Al only appeared the cubic phase, while CdS:Pb/CdS:Al homojunction mixed structure containing two phases: hexagonal and cubic. It's challenging to determine whether the (111), (220), and (311) peaks belong to the cubic phase or (002), (110), and (112) peaks belong to the hexagonal phase.

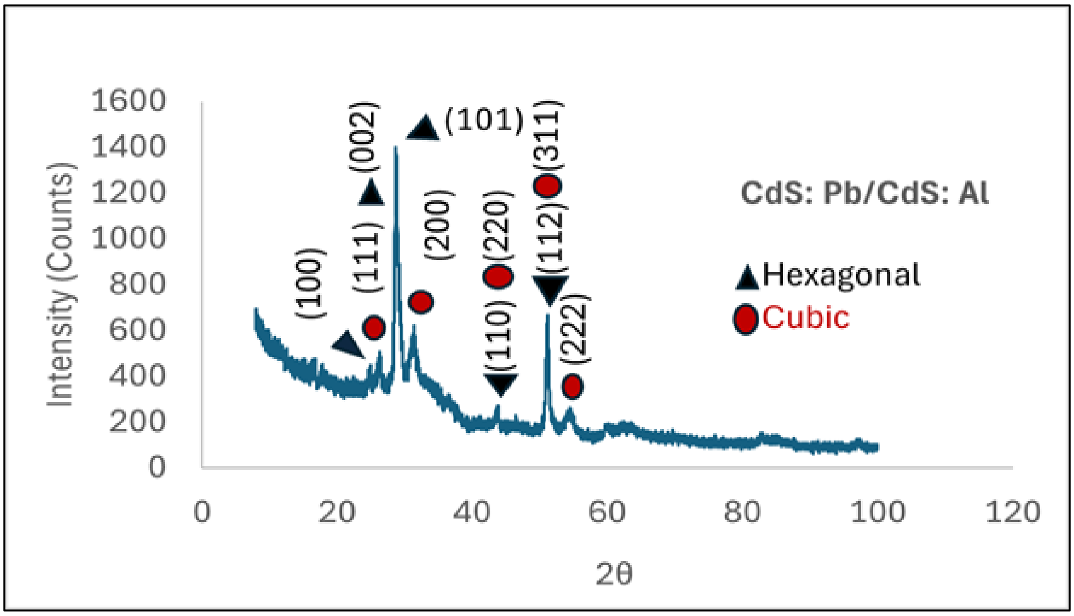

Figure 3. patterns of XRD for CdS: Pb/ CdS: Al homojunction at concentration of 0.002M.

The average crystalline size, Dhkl, of the pure CdS film, CdS films doped with Pb and Al, as well as CdS:Pb/CdS:Al homojunction films was calculated using Debye–Scherrer formula (Shanmugariya & Sakthivel, 2020) corresponding to highest diffraction peaks (111) and listed in table (1).

$$D = \frac{K\lambda}{\beta Cos\,\theta} \quad \ldots\ldots\ldots\ldots\ldots\ldots\ldots\ldots (3)$$

Where λ represents the wavelength of the X-ray (λ = 0.15406 μm), ϴ represents Bragg angle and β represents the FWHM (in radians).

It was found a significant decrease in the crystalline size was calculated based on the diffraction peak (111) of doped films as shown in table (1). In general, there is no significant change in the crystallite size calculated on the diffraction peak (111) of the Pb and Al films prepared at concentration ranging from 0.004M to 0.006M.

Table 1. XRD data of undoped CdS, (Pb, Al)-doped CdS and CdS: Pb/CdS: Al homojunction thin films.

System	(hkl)	d-spacing of plane	Crystalline size (nm)
CdS	(111)	3.30304	38.9
CdS: Pb 0.002M	(111)	3.39483	9.1
CdS: Pb 0.004M	(111)	3.4005	0.8
CdS: Pb 0.006M	(111)	3.50358	1.8
CdS: Al 0.002M	(111)	3.1807	2.7
CdS: Al 0.004M	(111)	3.38464	1.9
CdS: Al 0.006M	Amorphous	----	----
CdS: Pb/CdS:Al	(101)	3.098	9.4

3.2. Film morphology

The FE-SEM images of undoped CdS film, (Pb, Al)-doped CdS and CdS: Pb/ CdS:Al homojunction deposited at 70°C for two hours are shown in Figure 4. It was seen that undoped film had spherical shapes contain clusters and compact without cracks on the surface. The images of FE-SEM show that (Pb, Al)- doping did have plays an essential role in shaping morphological structure of CdS film. We can see from the FE-SEM pictures that films doped with concentration 0.002M of Pb and Al formation of agglomerated nanoparticles as shown in Figure 4. For concentration 0.004M of Pb and Al growth of agglomerated nanoparticles, where some of the clusters coalesce forming bigger agglomerates in different shapes and orientation. The doped CdS film with Pb and Al resultig in stress in the CdS films is directly attributable to surface defects present on them, this is also evident from the change in peak intensity in the XRD pattern with increasing doping ratios of Pb and Al. The average grains diameters of doped films and undoped film range from 23.92nm to 274.1nm.

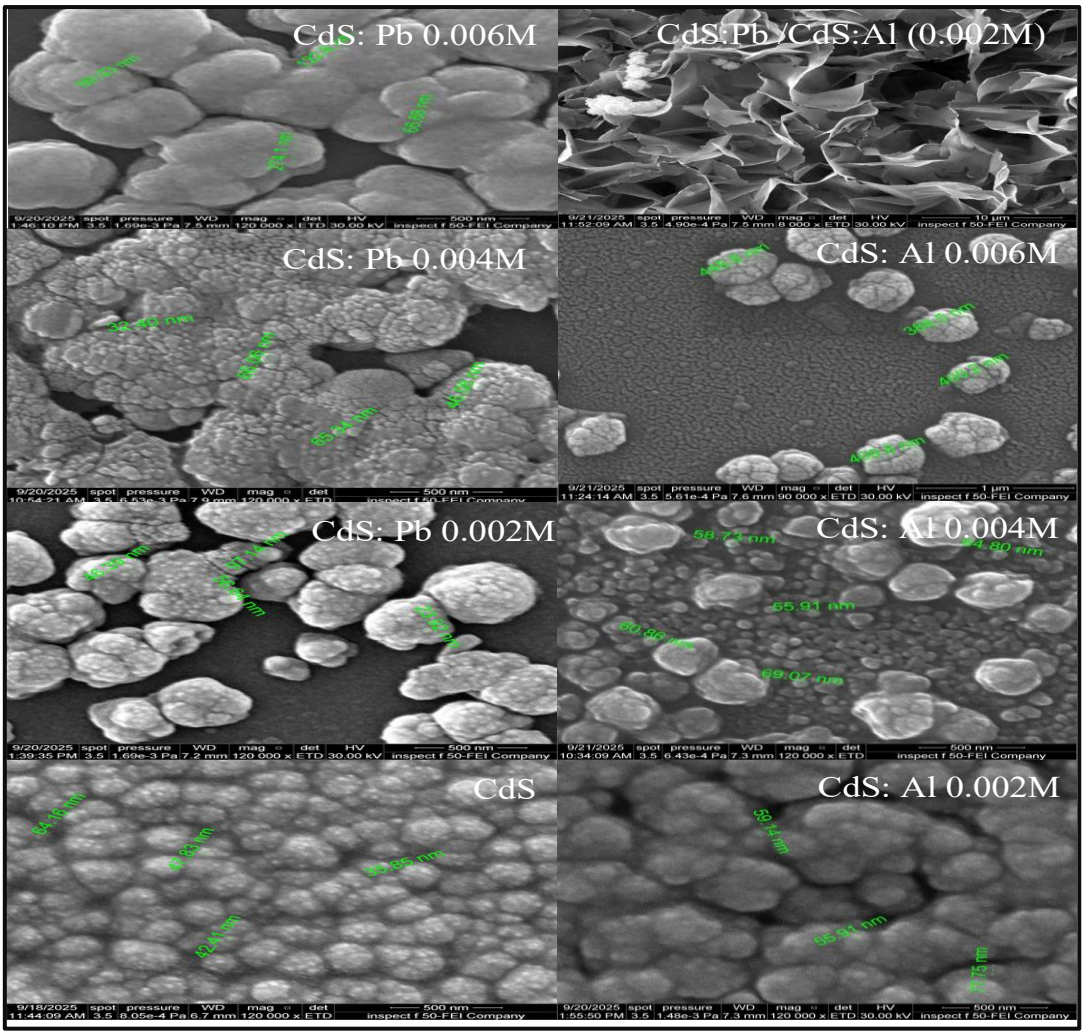

Figure 4. FE-SEM of undoped CdS film, (Pb, Al)-doped CdS at various concentrations and CdS: Pb/CdS: Al homojunction.

Average CdS: Pb/CdS: Al homojunction films thickness was obtained by SEM cross-section as shown in Figure 5. The resulting thicknesses value is 15.22 μm.

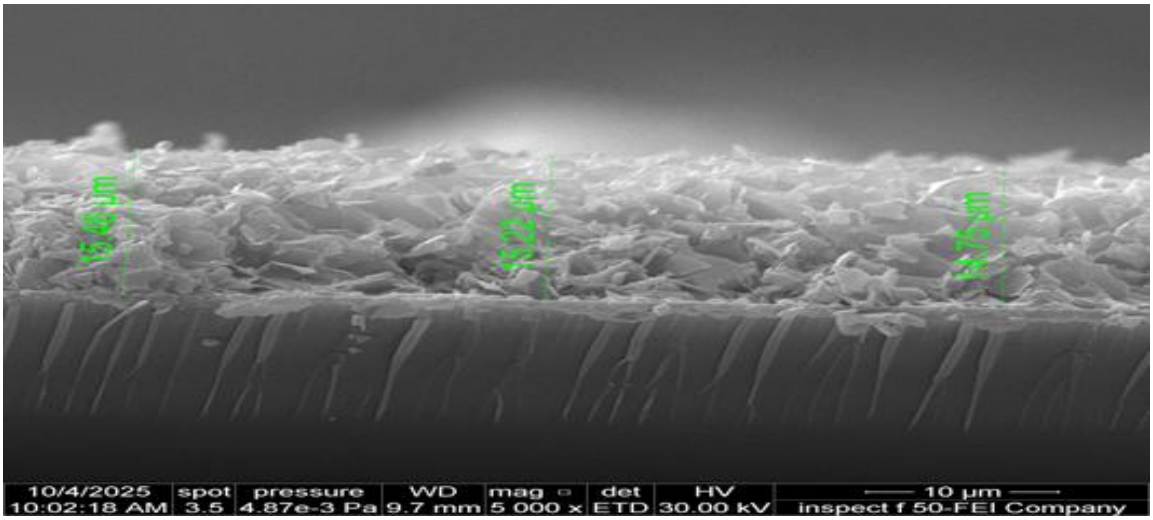

Figure 5. SEM cross-section of CdS: Pb/ CdS: Al homojunction film.

3.3. Compositional analysis

The quantitative composition of elementals for the pure CdS film and CdS films doped with different concentrations of Pb and Al (0.002M, 0.004M and 0.006M) as well as CdS: Pb/ CdS: Al homojunction film were detected using an energy dispersive spectrometer of Cd, Pb, Al and S elements are summarized in table 2. The EDX analysis showed the existence of Cd, S, Pb and Al as the main constituent elements of the sample as illustrated in Figure 6. The pure CdS thin film is characterized by their high sulfur content, while thin films doped with Pb and Al, the sulfur content deficient which increases the semiconducting nature of the material. That the sulfur deficient when Pb and Al doped CdS films shows high gas sensing performance of the films.

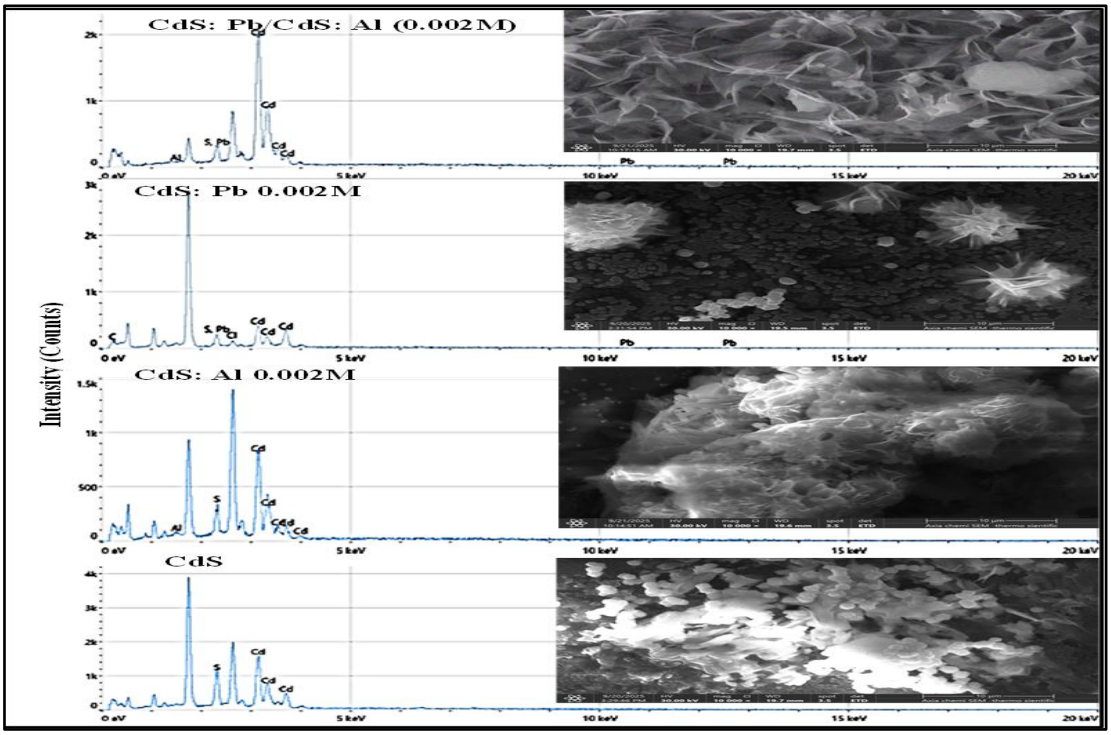

Figure 6. EDX spectra of pure CdS, CdS: Pb 0.002M, CdS: Al 0.002M and CdS: Pb/ CdS: Al homojunction thin films.

Table 2. XRD data of pure CdS, CdS: Pb 0.002M, CdS: Al 0.002M and CdS: Pb/ CdS: Al homojunction thin films.

System	Elements			
	Cd	S	Pb	Al
	Weight%			
Undoped	79.9	20.1	0	0
CdS; Pb 0.002M	80.1	19.6	0.3	
CdS: Al 0.002M	84.5	11.6	0	3.9
CdS:Pb/CdS:Al (0.002M)	84.2	3.2	0.7	0.5

3.4. Gas sensing

The sensitivity of the pure CdS thin film and CdS films doped with varying concentrations of Pb and Al (0.002M, 0.004M and 0.006M) as well as CdS: Pb/ CdS: Al homojunction film are studied by optimizing of the work condition to achieve the lowest operating temperature. The thin films were initially investigated to confirm their semiconducting behavior. The sensor is placed in a vacuum chamber on heater base and its electrical resistance is measured as the temperature is risen up from RT to 300°C in the clean dry air. The sensing test was done under fixed concentration of NO2 and H2S and bias 6v were applied on the electrodes of all these films. It is inferred from table (3) that the sensing respons of H2S and NO2 increases continuously with increasing concentration up to the maximum value at concentration of 0.004M. To optimize the operating temperature of Pb-doped and undoped thin films were subject to different temperature (100-300°C) of the H2S and NO2 gas at 100 ppm. It was noticed from table (3) the CdS: Pb (0.004M) sensor exhibits maximum sensitivity estimated at approximately 175.2% and 48.31 at operating temperature of 300°C respectively as compared to undoped [11.22%], CdS: Pb (0.002M)[111.4%] and CdS: Pb (0.006M) [12.42%] for H2S gas, there while for NO2 gas was undoped [14.21%], CdS: Pb (0.002M)[20.77%] and CdS: Pb (0.006M)[41.38%]. Accordingly, a temperature 300°C was adopted as optimum temperature for studding the sensing of H2S and NO2 gases for CdS: Pb (0.004M). To optimize the operating temperature of CdS thin film doped with Al were subject to different temperature (100-300°C) of the H2S and NO2 gas at 100 ppm. It was noticed from table (3) the CdS: Al (0.004M) sensor exhibits maximum sensitivity estimated at approximately 54,15% at operating temperature of 200°C, while for NO2 gas 44.96% at operating temperature of 300°C , as compared to undoped [11.22%], CdS: Al (0.002M)[16.69%] and CdS: Al (0.006M) [24.93%] for H2S gas, there while for NO2 gas was undoped [14.21%], CdS: Al (0.004M)[35.2%] and CdS: Al (0.006M)[13.24%]. Therefore, a temperature 300°C was adopted as optimum temperature for studding the sensing of H2S gas for CdS: Al (0.004M).

The CdS:Pb thin films at concentration (0.004M) exhibits the maximum sensitivity of (175.2%) towards 100 ppm H2S gas at operating temperature of 300°C can be explained depending of surface nature, lattice defects, grain size, oxygen adsorption and porous nature which leading increasing in more active sites and provide larger surface area for gas diffusion, and with high porosity, it contributes to greater number of gas molecules adsorbed on the surface of the film (Gawali, Patil, Deonikar, Patil, Patil, Patil, & Pant, 2018).

Table 3. Sensitivity behavior at different operation temperature of undoped CdS, (Pb, Al)-doped CdS and CdS: Pb/ CdS: Al homojunction thin films.

System	Sensitivity(S%)			Sensitivity(S%)		
	Gas H_2S			Gas NO_2		
	Operation temperature (°C)			Operation temperature (°C)		
	100	200	300	100	200	**300**
CdS	0	10.98	11.22	0	4.86	**14.21**
CdS: Pb 0.002M	0	0	111.4	0	0	**20.77**
CdS: Pb 0.004M	0	0	175.2	0	0	**48.31**
CdS: Pb 0.006M	9.27	7.17	12.42	25.46	40.47	**41.38**
CdS: Al 0.002M	21.93	16.69	27.55	5.36	33.70	**44.96**
CdS: Al 0.004M	37.95	54.15	37.50	27.18	35.2	**12.59**
CdS: Al 0.006M	24.64	24.93	5.293	13.08	13.24	**9.196**
CdS: Pb/CdS:Al	22.62	28.84	19.65	14.18	17.12	**14.67**

3.5. Response and recovery time

From table 4 the response and recovery time of the pure CdS film and CdS films doped with different concentrations of Pb and Al (0.002M, 0.004M and 0.006M) as well as CdS: Pb/CdS: Al homojunction film at operating temperature for 100ppm concentration of H2S and NO2 gas. The sensor is characterized by its fast response for H2S and NO2 gas at 100 ppm concentration for CdS:Pb 0. 004 M but the recovery time will be longer. For H2S gas, the CdS:Pb 0.004M thin film has response time of 8.1s with recovery time of 62.1s, but upon contact with NO2 gas, the response time of 20.7s with the recovery time of 64.8s. For CdS:Al 0.002M thin film exhibits rapid performance of response time with recovery time exposure to H2S, while CdS:Al 0.006M has faster response 13.5s but a longer recovery time 102.6s. the CdS:Pb/CdS:Al sensor has response time of 20.7s with recovery time of 66.6s for H2S, when exposed to NO2 gas a response time of 28.8s with recovery time of 60.3s . These results indicate that the CdS:Pb 0.004M thin film demonstrates higher efficiency in sensing H2S gas compared to NO2 gas and also registers a greater sensing response towards H2S gas.

Table 4. Results of response and recovery time at operating temperature for pure CdS film and CdS films doped with Pb and Al, as well as CdS: Pb/CdS: Al homojunction film.

System	Response time(s)		Recovery time(s)	
	H_2S	NO_2	H_2S	**NO_2**
CdS	9.9	21.6	76.5	**66.6**
CdS: Pb 0.002M	8.1	26.1	61.2	**63**
CdS: Pb 0.004M	8.1	20.7	62.1	**64.8**
CdS: Pb 0.006M	18.9	22.5	71.1	**45.9**
CdS: Al 0.002M	9	16.2	56.7	**52.2**
CdS: Al 0.004M	13.5	19.8	99.9	**66.6**
CdS: Al 0.006M	16.2	13.5	70.2	**102.6**
CdS: Pb/CdS:Al	20.7	28.8	66.6	**60.3**

3.6. Sensing mechanism

The sensing mechanism in the present study can be explained as follows, when the thin films are exposed to air, oxygen molecules are physiosorbed flowed by its chemisorption's on the film surface at high temperature (Kamble, Harale, Patil, Patil, & Kadm, 2017). The sensing property of thin film is beginning upon adsorption of oxygen molecules from the atmosphere, then capture the electrons in the conduction band, which leads to ionosorption as atomic () and molecular () species depending operating temperature (Ganesh et al., 2017).

Figure 7. illustrates the dynamic response to Hydrogen sulfide and Nitrogen dioxide gas of the pure CdS film and CdS films doped with Pb and Al. The results clearly indicate that resistance of the undoped CdS thin film is increases during exposure to reducing gas, while during exposure to an oxidizing gas, the resistance reduced, indicating that the material behaves as p-type semiconductors. In contrast, the resistances of Pb-doped CdS thin films with concentration of 0.002M, 0.004M and 0.006M are decreases during exposure to reducing gas, while during exposure to an oxidizing gas, the resistance increased, this indicates that the material demonstrating a n-type semiconductor behavior. Thus, the presence of Pb in the CdS thin films leads to reversal of electrical properties for CdS thin films as illustrate in Figure 7.

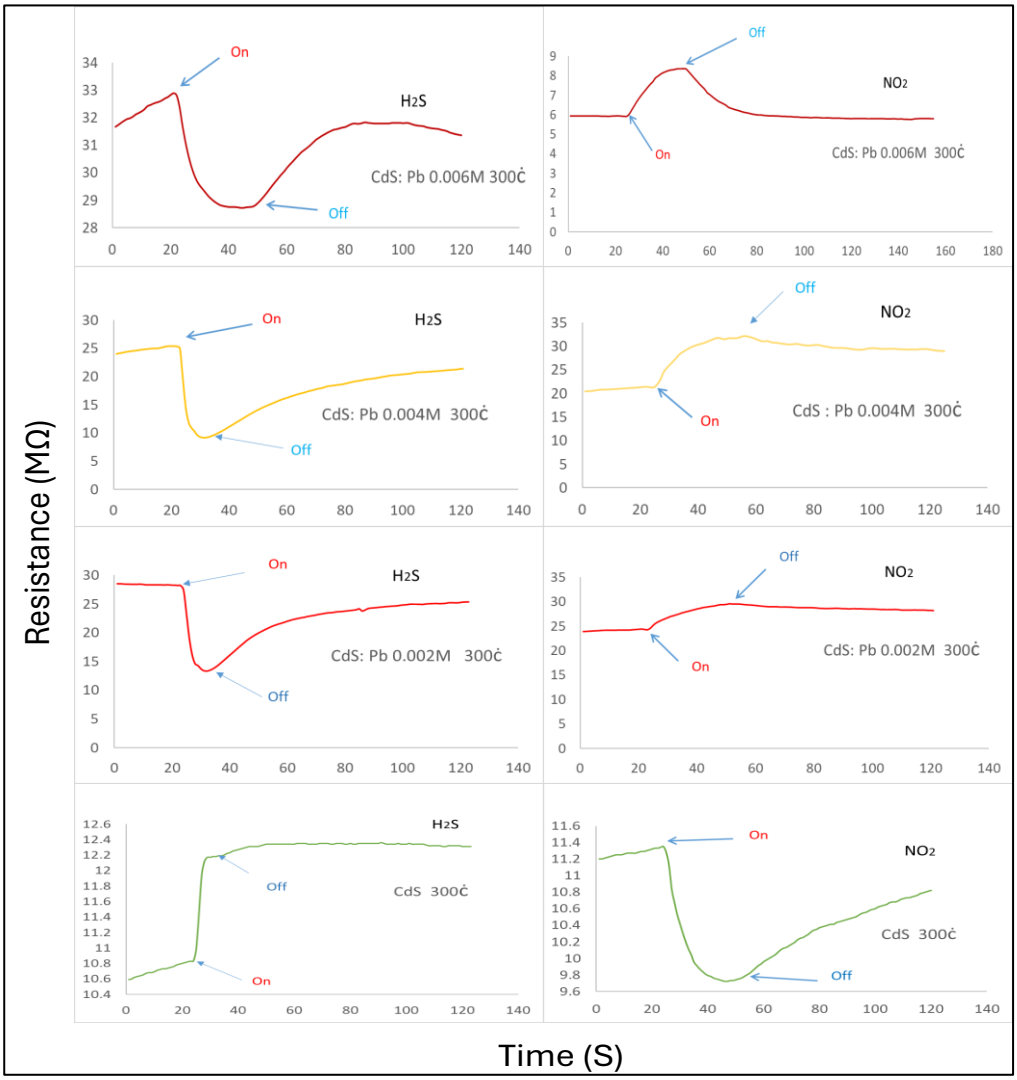

Figure 7. variation in resistance of sensor CdS thin film and CdS: Pb as function of time at different concentration.

when Al-doped CdS thin film does not lead to an inversion of the behavior of p-type for the CdS semiconductor, also CdS:Pb/CdS:Al sensor as shown in Figure 8 and 9 respectively. Oxygen molecules adsorption on the sensor surface in n-type semconductors acts as trap for conduction band electrons, thereby reducing the electron concentration and leading to the formation of depletion region; therefore, the electrical conductivity of the sensor is reduced to a minimum. Hydrogen sulfide is a reducing gas that interacts with chemisorbed oxygen species and readily oxidizes into SO2, H2O and electrons. This means that the H2S gas act as electron donors, transferring electrons to the conduction band of Pb-doped CdS. The response to H2S can be explained as a reaction of gas with to O2(ads) (Patil, Kajale, Chavan, Pawar, Ahire, Shinde, Gaikwad, & Jain, 2011).

$$H_2S + 3O_{(ads)^-} \rightarrow H_2O_{(g)} + SO_{2\ (g)} + 3e^- \ldots\ldots\ldots\ldots\ldots\ldots\ldots\ldots\ldots\ldots\ldots\ldots\ldots\ldots (4)$$

Thus, this leads to increased electron concentration and the resistance of sensor decreased as shown in Figure 7.

After exposing Pb-doped CdS thin films to Nitrogen dioxide gas, due to oxidizing nature NO2 gas, readily reaction between the NO2 molecule and ionosorbed oxygen ions, which causes the formation of adsorbed as shown in equation (Jagadale, Patil, Vanalakar, Patil, & Deshmukh, 2018).

$$NO_{2\ (gas)} + e^- \rightarrow NO_{2\ (adsorbed)}^- \ldots\ldots\ldots\ldots\ldots\ldots\ldots\ldots\ldots\ldots\ldots\ldots\ldots\ldots\ldots\ldots\ldots\ldots (5)$$

$$NO_{2\,(gas)} + O_{2\,(adsorbed)}^- + 2e^- \rightarrow NO_{2\,(adsorbed)}^- + 2e_{(adsorbed)}^- \ldots\ldots\ldots\ldots (6)$$

Because capture electrons directly from conduction band of Pb-doped CdS, the concentration of hole increases that further lead to the increase in resistance as shown in Figure 7.

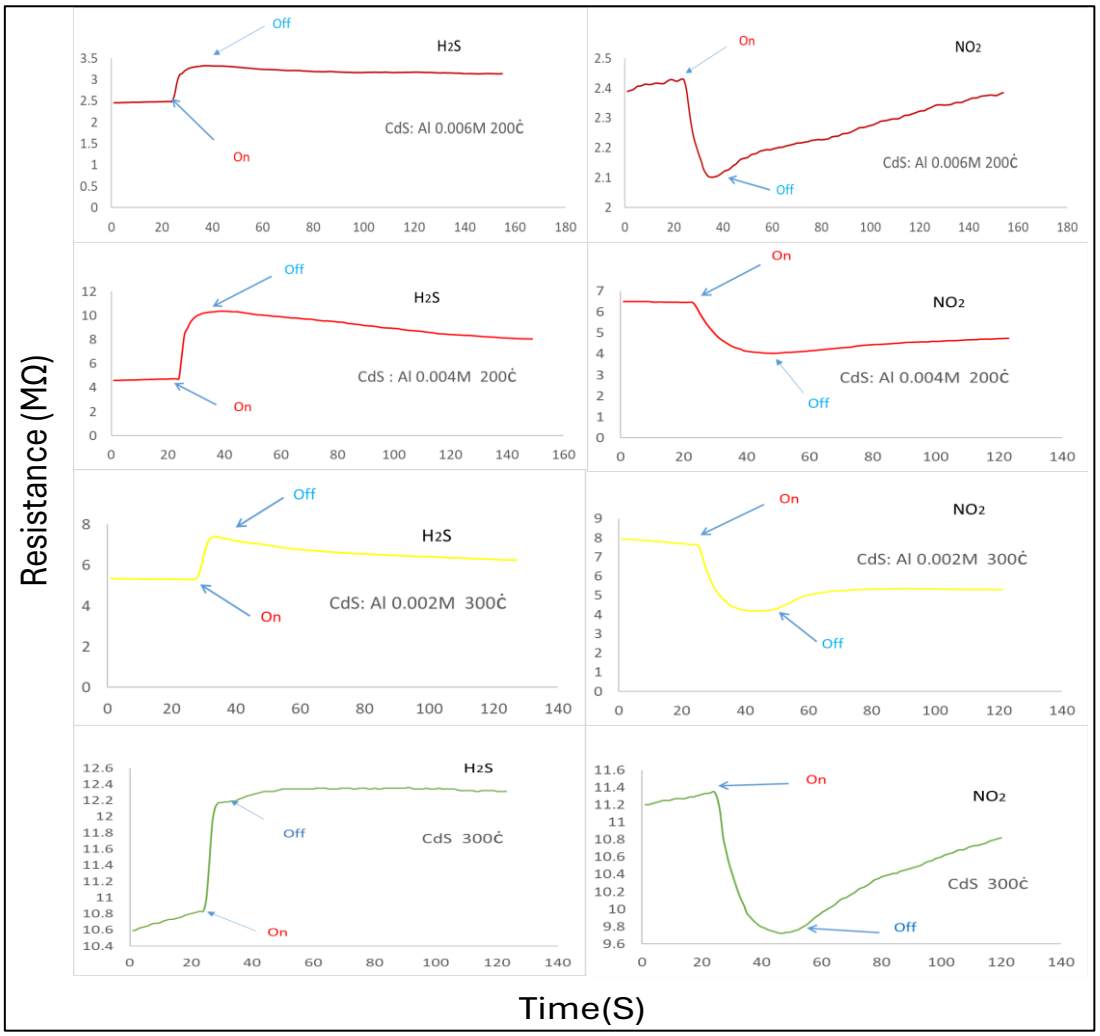

Figure 8 variation in resistance of sensor CdS: Al as function of time at different concentration.

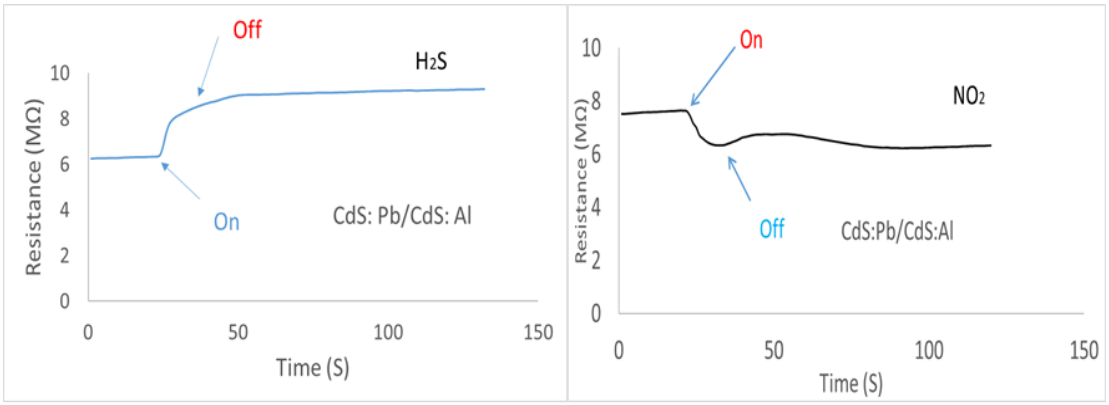

Figure 9 variation in resistance of sensor CdS: Pb/CdS: Al homojunction as function time.

4. Conclusion

The pure CdS film and CdS films doped with varying concentrations of Pb and Al (0.002M, 0.004M and 0.006M) as well as CdS: Pb/ CdS: Al homojunction film were coated onto glass substrate via the chemical bath deposition method at deposition temperature of 70°C. Significant change of undoped CdS thin film is observed in crystal structure from mix phase of hexagonal and cubic to cubic

structure by doping of Pb and Al. Among these doped films, the Pb-doped CdS thin film at concentration of 0.004M, it features the highest sensitivity and best response times for both Hydrogen sulfide and Nitrogen dioxide gases when compared to the films doped at concentration of 0.002M and 0.006M. CdS gas sensors is display a P-type response towards H2S and NO2 gases, while Pb-doped CdS thin film display the N-type behavior of the CdS semiconductor.

References

Aliyu, M., Diso, D. G., Musa, A. O., & Abubakar, A. L. (2022). Effect of growth voltage on electrodeposited CdS thin films. *Bayero Journal of Pure and Applied Sciences*, *13*, 539–545.

An, B., Kim, H., Chang, Y. W., Park, J., & Pyun, J. (2021). Photosensors based on cadmium sulfide (CdS) nanostructures: A review. *Journal of the Korean Ceramic Society*, *58*(6), 631–644. https://doi.org/10.1007/s43207-021-00141-5

Ashok, A., Regmi, G., Romero-Nunez, A., Solis-Lopez, M., Velumani, S., & Castaneda, H. (2020). Comparative studies of CdS thin films by chemical bath deposition techniques as a buffer layer for solar cell applications. *Journal of Materials Science: Materials in Electronics*, *31*, 20460–20471. https://doi.org/10.1007/s10854-020-03024-3

Bari, R. H., Patil, S. B., & Bari, A. R. (2013). Spray-pyrolyzed nanostructured CuO thin films for H2S gas sensor. *International Nano Letters*, *3*(12). https://doi.org/10.1186/2228-5326-3-12

Batu, B., & Tamasgen, T. (2020). Effects of thickness on optical and structural properties of lead sulphide (PbS) thin film prepared by chemical bath deposition. *Chemistry and Materials Research*, *12*(7). https://doi.org/10.7176/CMR/12-7-01

Bettini, M., Bachmann, K. J., & Shay, J. L. (1978). CdS/InP and CdS/GaAs heterojunctions by chemical-vapor deposition of CdS. *Journal of Applied Physics*, *49*, 865–870. https://doi.org/10.1063/1.324617

Chavez-Urbiola, I. R., Pintor-Monroy, M. I., Willars-Rodriguez, J., & Quevedo-Lopez, Y. V. (2019). Effects of aluminum doping upon properties of cadmium sulfide thin films and its effect on ITO/CdS:Al/NiOx/Ni/Au diodes. *Journal of Applied Physics*, *126*. https://doi.org/10.1063/1.5087153

Diwate, K., Pawbake, A., Rondiya, S., Kulkarni, R., Waykar, R., Jadhavar, A., Rokade, A., Funde, A., Mohite, K., Shinde, M., Pathany, H., Devan, R., & Jadkar, S. (2017). Substrate temperature dependent studies on properties of chemical spray pyrolysis deposited CdS thin films for solar cell applications. *Journal of Semiconductors*, *38*, 023001. https://doi.org/10.1088/1674-4926/38/2/023001

Faraj, M. G., & Ibrahim, K. (2012). Comparison of cadmium sulfide thin films deposited on glass and polyethylene terephthalate substrates with thermal evaporation for solar cell applications. *Journal of Materials Science: Materials in Electronics*, *23*, 1219–1223. https://doi.org/10.1007/s10854-011-0576-6

Ferra-Gonzalez, S. R., Berman-Mendoza, D., Garcia-Gutierrez, R., Castillo, S. J., Ramirez-Bon, R., Gnade, B. E., & Quevedo-Lopez, M. A. (2014). Optical and structural properties of CdS thin films grown by chemical bath deposition doped with Ag by ion exchange. *Optik – International Journal of Light and Electron Optics*, *125*, 1533–1536.

Ganesh, R. S., Durgadevi, E., Navaneethan, M., Patil, V. L., Ponnusamy, S., Muthamizhchelvan, C., Kawaski, S., Patil, P. S., & Hayakawa, Y. (2017). Low temperature ammonia gas sensor based on Mn-doped ZnO nanoparticle decorated microspheres. *Journal of Alloys and Compounds*, *721*, 182–190. http://dx.doi.org/10.1016/j.jallcom.2017.05.315

Gawali, S. R., Patil, V. L., Deonikar, V. G., Patil, S. S., Patil, D. R., Patil, P. S., & Pant, J. (2018). Ce doped NiO nanoparticles as selective NO2 gas sensor. *Journal of Physics and Chemistry of Solids*, *114*, 28–35. https://doi.org/10.1016/j.jpcs.2017.11.005

Hasanirokh, K., Asgari, A., & Mohammadi, S. (2021). Fabrication of light-emitting device based on the CdS/ZnS spherical quantum dots. *Journal of the European Optical Society Rapid Publications*, *17*(1). https://doi.org/10.1186/s41476-021-00173-8

Jagadale, S. B., Patil, V. L., Vanalakar, S. A., Patil, P. S., & Deshmukh, H. P. (2018). Preparation, characterization of 1D ZnO nanorods and their gas sensing properties. *Ceramics International*, *44*, 3333–3340. https://doi.org/10.1016/j.ceramint.2017.11.116

Jafari, A., Zakaria, A., Rizwan, Z., & Ghazali, M. S. M. (2011). Effect of low concentration Sn doping on optical properties of CdS films grown by CBD technique. *International Journal of Molecular Sciences*, *12*, 6320–6328. https://doi.org/10.3390/ijms12096320

Kamble, D. L., Harale, N. S., Patil, V. L., Patil, P. S., & Kadm, L. D. (2017). Characterization and NO2 gas sensing properties of spray pyrolyzed SnO2 thin films. *Journal of Analytical and Applied Pyrolysis*, *127*, 38–46. https://doi.org/10.1016/j.jaap.2017.09.004

Liu, F., Lai, Y., Liu, J., Wang, B., Kuang, S., Zhang, Z., Li, J., & Liu, Y. (2010). Characterization of chemical bath deposited CdS thin films at different deposition temperature. *Journal of Alloys and Compounds*, *493*(1–2), 305–308. https://doi.org/10.1016/j.jallcom.2009.12.088

Muthusamy, M., Muthukumaran, S., & Ashokkumar, M. (2014). Composition dependent optical, structural and photoluminescence behavior of CdS:Al thin films by chemical bath deposition method. *Ceramics International*, *40*, 10657–10666. https://doi.org/10.1016/j.ceramint.2014.03.050

Patil, G. E., Kajale, D. D., Chavan, D. N., Pawar, N. K., Ahire, P. T., Shinde, S. D., Gaikwad, V. B., & Jain, G. H. (2011). Synthesis, characterization and gas sensing performance of SnO2 thin films prepared by spray pyrolysis. *Bulletin of Materials Science*, *34*(1), 1–9. https://doi.org/10.1007/s12034-011-0045-0

Paudel, N. R., Wieland, K. A., & Compaan, A. D. (2012). Ultrathin CdS/CdTe solar cells by sputtering. *Solar Energy Materials and Solar Cells*, *105*, 109–112. https://doi.org/10.1016/j.solmat.2012.05.035

Ramarj, S. G., Nundy, S., Zhao, P., Elanaran, D., Tahir, A. A., Hayakawa, Y., Muruganathan, M., Mizuta, H., & Kim, S.-W. (2022). RF sputtered Nb-doped MoS2 thin film for effective detection of NO2 gas molecules: Theoretical and experimental studies. *ACS Omega*, *7*, 10492–10501. https://doi.org/10.1021/acsomega.1c07274

Rondiya, S., Rokade, A., Gabhale, B., Pandharkar, S., Chaudhari, M., Date, A., Chaudhary, M., Pathan, H., & Jadkar, S. (2017). Effect of bath temperature on optical and morphology properties of CdS thin films grown by chemical bath deposition. *Energy Procedia*, *110*, 202–209.

Shanmugariya, S., & Sakthivel, B. (2020). ZnSe/CdS thin films prepared with physical vapor deposition technique. *Adalya Journal*, *9*, 635–640.

Soonmin, H. (2021). Deposition of metal sulphide thin films by chemical bath deposition technology: Review. *International Journal of Thin Films Science and Technology*, *10*(1), 45–57. https://doi.org/10.18576/ijtfst/100108

Toma, F. T. Z., Hussain, K. M. A., Rahman, M. S., & Syed. (2021). Preparation and characterization of CdS thin film using chemical bath deposition (CBD) technique for solar cell application. *World Journal of Advanced Research and Reviews*, *12*(3), 629–633. https://doi.org/10.30574/wjarr.2021.12.3.0746

Tyagi, V. V., Rahim, N. A. A., Rahim, N. A., & Selvaraj, J. A. (2013). Progress in solar PV technology: Research and achievement. *Renewable and Sustainable Energy Reviews*, *20*, 443–461. https://doi.org/10.1016/j.rser.2012.09.028

Verma, M. K., & Gupta, V. (2012). A highly sensitive SnO2-CuO multilayered sensor structure for detection of H2S gas. *Sensors and Actuators B: Chemical*, *166–167*, 378–385. https://doi.org/10.1016/j.snb.2012.02.076

Yin, Y., Shen, Y., Zhao, S., Li, A., Lu, R., Han, C., Cui, B., & Wei, D. (2022). Enhanced detection of ppb-level NO2 by uniform Pt-doped ZnSnO3 nanocubes. *International Journal of Minerals, Metallurgy and Materials*, *29*(6), 1295–1303. https://doi.org/10.1007/s12613-020-2215-9